

# Shortcut to adiabaticity in spin fragmented condensates

Author: David López Núñez.

*Facultat de Física, Universitat de Barcelona, Diagonal 645, 08028 Barcelona, Spain.\**

Advisor: Artur Polls and Bruno Julià-Díaz.

**Abstract:** We perform a method to shortcut the adiabatic evolution in spin-1 Bose gas with an external magnetic field as the control parameter. An initial state, easy to achieve experimentally, with almost all bosons in the Zeeman sublevel  $m = 0$ , is evolved to a final state very close to a macroscopic singlet. In order to apply the shortcut protocol, some approximations are made for obtaining an harmonic oscillator Hamiltonian, where this protocol can be applied. The shortcut method is compared to a linear variation of the control parameter as a test to prove its improvement in the construction of the final states.

## I. INTRODUCTION

Quantum cold gases have provided an excellent tool to study quantum properties at a macroscopic level. For both bosons and fermions, it has been possible to produce controlled many-body correlated quantum states. Boson gases at low enough temperatures tend naturally to form Bose-Einstein condensates (BEC). BEC's are systems where a macroscopic amount of atoms occupy the same single-particle state. There are situations where simultaneous macroscopic occupations of different single-particle states occur, producing a fragmented condensate. This fragmentation can be caused by different reasons such as internal (internal Josephson junctions) or orbital (Bose gases in optical lattices) degeneracies [1].

A spin-1 Bose gas is a trapped Bose-Einstein condensate in which atoms can populate three hyperfine states [2]. In the antiferromagnetic case, with repulsive interactions, the macroscopic ground state of the system is a singlet. Under the action of an external magnetic field, the ground state is modified. While the linear term of the magnetic field only shifts the energy, the quadratic Zeeman (QZ) effect plays a key role in the determination of the equilibrium state. This interaction between the atoms and the external field favours an unfragmented condensed state, with all atoms with the third component of spin along the field direction equal to zero.

There is a huge experimental interest in preparing the singlet state, which means total spin  $S = 0$ . Unfortunately, it is not easy to achieve. However, a condensate with its total third component  $M = 0$ , but not a singlet, has been already performed [3]. Therefore, setting this last state at the beginning of the experimental preparation and slowly decreasing the magnetic field, one could adiabatically arrive to the singlet state. However, it is of a high interest to develop methods for producing macroscopic quantum states in small time intervals, by shortcutting the adiabatic following [4, 5]. The process we propose can be used for the spin-1 Bose gas allowing the

fast production of these states.

The shortcut protocols respond to the necessity of producing controlled quantum states efficiently in a finite time. These protocols manage to arrive to a desired final state, which is usually the ground state of the system, in a shorter time than if the adiabatic evolution would have been followed.

The adiabatic following implies very small variations of a control parameter over time. Therefore, the system is able to adapt to such slow modifications, so that it is always in the ground state of the Hamiltonian. The shortcut protocol, on the other hand, consists on changing the control parameter in such a way that at the end of the evolution, the system arrives to the same final state in a shorter time. The process, then, does not follow the adiabaticity, so the system is not always in the instantaneous ground state of the Hamiltonian. However, at the final time, the protocol arrives to the same state than the obtained with the adiabatic evolution but much faster, which makes this method very efficient. It is also possible to control or limit other quantities during the evolution, such as setting a maximum energy during all the process, reducing the noise excitations...

In this study, a shortcut protocol already known for an harmonic oscillator will be adapted for an approximated Hamiltonian of a spin-1 Bose gas. This method implies controlling the external magnetic field over time, which is experimentally easy to perform, being the QZ energy our control parameter. We will set as our initial state a ground state very close to a BEC with total  $M = 0$ , which has been already produced in previous experiments. By using the shortcut protocol, the QZ energy will be modified in order to produce a final state similar to the singlet state, which is the ground state in absence of a magnetic field. The main purpose is, therefore, to produce this last state with good precision the fastest as possible.

The paper is organized as follows. In section II, a theoretical approach to the system is presented. First, we will explain the mathematical tools necessary to justify our approximations until reaching the desired harmonic Hamiltonian, for which already exist shortcut protocols. An explanation of the shortcut protocol will be also made. Section III contains a brief comparison be-

---

\*Electronic address: [dln@ecm.ub.edu](mailto:dln@ecm.ub.edu)

tween the exact and the approximated equations. Then, results of the shortcut protocol will be compared to a linear variation of the control parameter. In the end of the section, some realistic values results are shown. Conclusions will be given in section IV.

## II. THEORETICAL MODEL

### A. Description of the system

Our system is an ultracold gas of spin-1 bosons in a trap under the action of an external magnetic field. We assume a single mode in the trap, that is, all bosons condense in the same spatial orbit irrespective of their internal state. Therefore, there are only three single-particles states,  $|+1\rangle$ ,  $|0\rangle$  and  $|-1\rangle$ , corresponding to the Zeeman component  $m = +1, 0, -1$  respectively. The linear Zeeman effect acts only as a shift in the energy and does not contribute to determine the equilibrium state. The main contribution of the magnetic field is the quadratic, or second order, Zeeman (QM) effect. The system is thus well described by the Hamiltonian [2]

$$\frac{\hat{H}}{\hbar} = \frac{U_S}{2N} \hat{S}^2 - q \hat{N}_0, \quad (1)$$

where  $U_S > 0$  is the spin interaction term,  $N$  is the number of atoms,  $\hat{S}^2$  is the total spin operator,  $q$  is the quadratic Zeeman energy and  $\hat{N}_i$  is the number operator of the Zeeman state  $i$  ( $0, \pm 1$ ).

In this Hamiltonian there are only two terms that compete. The first one is caused by the antiferromagnetic interactions between two atoms,  $U_{12} = g_S \mathbf{s}_1 \cdot \mathbf{s}_2$  with  $\mathbf{s}_i$  being the spin of the particle  $i$  ( $g_S > 0$ ). The density and momenta of BEC are so little that there is no need of including three-particle interaction corrections because such collisions are highly improbable. On the other hand, the other piece of the Hamiltonian is due to the interaction of the atoms with the external magnetic field. The linear effect of the magnetic field shifts the energy of the Zeeman sublevels  $m = \pm 1$  by the same value but opposite sign. In our case, which will be  $M = 0$  as we will explain later, it gives a null contribution to the total energy and can be omitted from the Hamiltonian. The same cannot be applied to the QZ effect, which has the form  $q(m^2 - 1)$  for each atom. Looking at this expression, one sees that only the particles with zero third component of spin contribute to the energy, with a negative value of  $-q$ . Both  $+1$  and  $-1$  Zeeman components of the spin give a null contribution in this expression. Actually, it is the level with  $m = 0$  that does not change the energy. However, rewriting the QZ effect in this way allows to write the many particle expression of this interaction as  $-q \hat{N}_0$ .

Case	$U_S$ -dominated	$q$ -Dominated
Limit	$U_S \gg qN$	$U_S \ll qN$
Ground State	Fragmented Condensate	Unfragmented Condensate
	$ N, S, M\rangle =  N, 0, 0\rangle$	$ \phi\rangle = \left(a_0^\dagger\right)^N  vac\rangle$

Table 1. The ground states of the different limiting cases.

There are two limit cases for this Hamiltonian (see Table 1), when either the inter-atomic interaction is zero or when there is no magnetic field applied. For the last situation, which means  $q = 0$ , the Hamiltonian is ruled by the total spin operator. In such case, the system tries to minimize the total spin by coupling all pairs to spin zero.

In the two particle case, the ground state is given by the singlet of two particles,  $|s\rangle \equiv \left((\hat{a}_0^\dagger)^2 - 2\hat{a}_{+1}^\dagger \hat{a}_{-1}^\dagger\right) |vac\rangle$  where the two atoms are coupled to total spin 0. Therefore, the many-body ground state is  $|s\rangle^{\otimes N/2}$ , for  $N$  even. This state has three macroscopically populated states, as  $\langle N_{+1}\rangle = \langle N_0\rangle = \langle N_{-1}\rangle = N/3$ . When simultaneous macroscopic occupations of single-particle states happen, the system is called a fragmented condensate.

On the contrary, when the interactions between particles can be neglected, the Hamiltonian is  $q$  dominated. The QZ effect makes all spins to change into the  $m = 0$  Zeeman component. The total ground state is a BEC of the form  $|0\rangle^{\otimes N}$ . Such a state has  $\langle N_0\rangle = N$  and  $\langle N_{+1}\rangle = \langle N_{-1}\rangle = 0$ , so it is an unfragmented condensate.

Experimentally, this second ground state is the easiest to prepare. Then, the evolution proposed for this system will be from the  $q$ -dominated state, where a strong magnetic field will be required, to a situation where it is almost zero.

When  $q$  vanishes, the eigenstates are known analytically and are given by the total spin eigenstates  $|N, S, M\rangle$ , where  $S$  is the total spin and  $M$  the total projection of  $S$  in the  $z$ -axis direction. During all the study, this basis will be used. A general state  $\phi_M$  will be then written as,

$$|\phi_M\rangle = \sum_{S=|M|}^N c_S |N, S, M\rangle. \quad (2)$$

It is worth noting that  $M$  keeps fix when changing  $q$ , because the Hamiltonian commutes with the total spin third component operator. This is a good approximation to the real behaviour due to the experimental conditions of the atomic quantum gases, which are highly isolated from the environment, and to the microscopic rotational invariance of spin exchange interaction. For practical convenience, from now on  $N$  will be set to an even number.

The construction of these states is not trivial and they

are built as follows [2],

$$|N, S, M\rangle = \frac{1}{\mathcal{Z}(N, S, M)^{1/2}} (\hat{S}_-)^P (\hat{A}^\dagger)^Q (\hat{a}_{+1}^\dagger)^S |vac\rangle, \quad (3)$$

where  $P = S - M$ ,  $2Q = N - S$ ,  $\hat{a}_i^\dagger$  and  $\hat{a}_i$  are the creation and annihilation operators of the state  $i$  respectively,  $\hat{S}_- = \sqrt{2}(\hat{a}_{-1}^\dagger \hat{a}_0 + \hat{a}_0^\dagger \hat{a}_{+1})$  is the lowering total spin operator and  $\hat{A}^\dagger = (\hat{a}_0^\dagger)^2 - 2\hat{a}_{+1}^\dagger \hat{a}_{-1}^\dagger$  is the singlet creation operator.

The expression of these states involves three operators. The first one,  $\hat{a}_{+1}^\dagger$  is the creation operator of a spin 1 particle with  $m = +1$ . This operator acting  $S$  times over the vacuum leads to the many-particle state  $|S, S, S\rangle$  (we are omitting constant multiplying factors). This state has  $S$  particles and both the total momentum and its projection over the z-axis are  $S$ . The following acting operators ( $\hat{A}^\dagger$  and  $\hat{S}_-$ ) commute with the total spin momentum operator and therefore do not modify this quantity, which is already the final one.

The singlet creator operator creates pairs with total spin 0, so it only changes the number of particles. Then, repeated actions of this operator add enough pairs so that the final number of particles is fulfilled, while both  $S$  and  $M$  remains unaltered. This leaves the state as  $|N, S, S\rangle$ . The number of pairs  $Q$  added has to follow the expression  $2Q = N - S$ . For the case where there is no magnetic field applied, this is the only operator involved in the expression of the ground state, which is  $(\hat{A}^\dagger)^Q |vac\rangle = |s\rangle^{\otimes Q}$ .

Finally, the only quantum number that has to be modified is  $M$ . For that, the lowering momentum operator  $S_-$  is used, as it reduces the third component by one unit while not modifying neither  $N$  nor  $S$ . The number of times  $P$  that this operator acts over the states has to fulfil the relation  $P = S - M$ . Hence, the final state  $|N, S, M\rangle$  is obtained, multiplied by a constant. The normalization factor has been analytically calculated using commutation relations and the few operators for which these states are eigenstates. The resulting factor is,

$$\mathcal{Z}(N, S, M) = S! \frac{(N - S)!!(N + S + 1)!!}{(2S + 1)!!} \frac{(S - M)!(2S)!}{(S + M)!}. \quad (4)$$

The action of the Hamiltonian in Eq. (1) over these states is also not easy to compute. Its first term, corresponding to the total spin momentum, is diagonal for the considered basis, as we are using eigenstates of the total spin momentum. However, it does not happen the same for the second piece, related to the quadratic Zeeman effect. The action of the operator  $\hat{N}_0 = \hat{a}_0^\dagger \hat{a}_0$  over the  $|N, S, M\rangle$  states requires some calculations, based again on operators whose action over these states is known and commutation relations.  $\hat{N}_0$  connects states with themselves and two by two, where the total spin  $S$  differs by two units. It means that the total Hamiltonian is tridiagonal in this basis and, therefore, easier to solve numer-

ically. The action of  $\hat{N}_0$  is [2],

$$\begin{aligned} q\hat{N}_0|N S M\rangle &= \\ &= q\sqrt{A_-(N, S + 2, M)A_+(N, S, M)}|N S + 2 M\rangle + \\ &+ q\sqrt{A_+(N, S - 2, M)A_-(N, S, M)}|N S - 2 M\rangle + \\ &+ q[A_-(N, S, M) + A_+(N, S, M)]|N S M\rangle, \end{aligned} \quad (5)$$

where

$$A_+(N, S, M) = \frac{(S + M + 1)(S - M + 1)(N - S)}{(2S + 1)(2S + 3)} \quad (6)$$

$$A_-(N, S, M) = \frac{(S + M)(S - M)(N + S + 1)}{(2S + 1)(2S - 1)}. \quad (7)$$

For simplicity,  $M = 0$  will be taken. As  $|M| \ll N$ , this assumption can be made and the results will not differ qualitatively. The results can be extrapolated to  $M \neq 0$  situations. From now on, the  $N$  index will be omitted, as it is a fixed quantity. Thus, every general state  $\phi$  is written as

$$|\phi\rangle = \sum_S c_S |S\rangle. \quad (8)$$

Combining these last results with the Schrödinger equation  $\hat{H}|\phi\rangle = E|\phi\rangle$  we arrive to the following discrete eigenvalue equation,

$$h_{S,S+2} c_{S+2} + h_{S,S-2} c_{S-2} + h_{S,S} c_S = E c_S, \quad (9)$$

with

$$\begin{aligned} h_{S,S+2} &= -q\sqrt{\frac{(N + S + 3)(N - S)}{(S + 1)(S + 2)}} \\ &\times \frac{1}{(2S + 3)\sqrt{(2S + 1)(2S + 5)}}, \\ h_{S,S-2} &= -q\sqrt{\frac{(N + S + 1)(N - S + 2)}{S(S - 1)}} \\ &\times \frac{1}{(2S - 1)\sqrt{(2S + 1)(2S - 3)}}, \\ h_{S,S} &= \frac{U_S}{2N} S(S + 1) \\ &- q \left[ \frac{S^2(N + S + 1)}{(2S - 1)(2S + 1)} + \frac{(S + 1)^2(N - S)}{(2S + 1)(2S + 3)} \right]. \end{aligned} \quad (10)$$

## B. Continuum approximation

There are well established shortcut protocols for one-body harmonic potentials. Therefore, it is convenient to explore the possibility to write our eigenvalue equation in such a way that known protocols can be applied. A first step is to transform Eq. (9) into a continuum approximation. Afterwards, some more justified simplifications on the system will be required until arriving to a harmonic shape of the Hamiltonian which will allow us to perform the shortcut protocol.

Some considerations can be made to the previous results. In the studied situation,  $1 \ll S \ll N$ . As long as

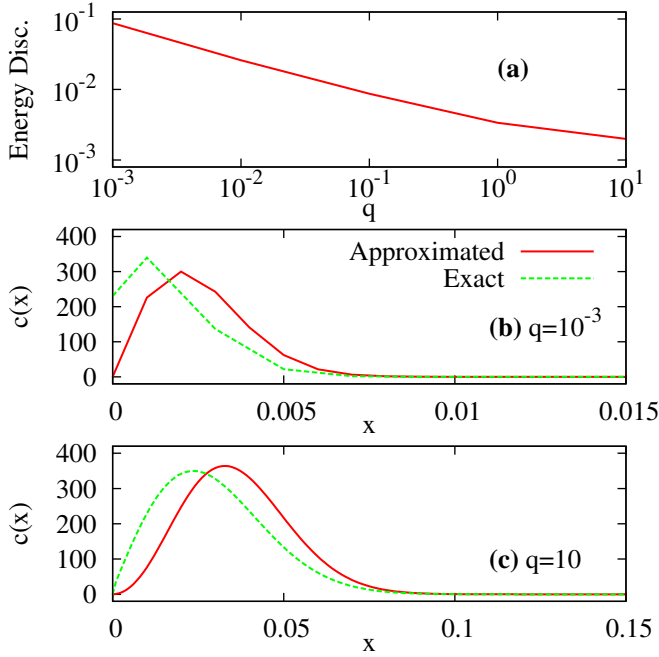


FIG. 1: In panel (a) energy discrepancy,  $|(E_{ex} - E_{ap})/E_{ex}|$ , of the ground states between the approximated and exact Hamiltonian is plotted for different values of  $q$ . Panels (b) and (c) show the ground state for the exact and approximated Hamiltonian for  $q = 10^{-3}$  and 10 respectively. Note the difference in the x axis for these two plots. For all these plots,  $N = 1000$  and  $U_S = 10$ .

$S$  is neither too large,  $S \sim N$ , nor too little  $S \sim 1$ ,  $c_S$  can be assumed to vary smoothly. Hence,  $c_S$  can be approximated to a continuous function  $c(x)$ , where  $x \equiv S/N$  and it varies from 0 to 1. Then,  $\epsilon = 2/N$  can be taken as a small parameter and a Taylor expansion is made,

$$c_{S \pm 2} = c(x) \pm \epsilon c'(x) + \frac{\epsilon^2}{2} c''(x) + \mathcal{O}(\epsilon^3). \quad (11)$$

This expression can be substituted into Eq. (9) and the following continuum Schrödinger equation is obtained

$$\alpha(x)c''(x) + \beta(x)c'(x) + (\gamma(x) - E)c(x) = 0, \quad (12)$$

where

$$\begin{aligned} \alpha(x) &= \frac{\epsilon^2}{2}(h_{S,S+2} + h_{S,S-2}), \\ \beta(x) &= \epsilon(h_{S,S+2} - h_{S,S-2}), \\ \gamma(x) &= h_{S,S} + h_{S,S+2} + h_{S,S-2}. \end{aligned} \quad (13)$$

Taking into account that  $1 \ll S \ll N$ , one can set the order until which we want to approximate. Performing Taylor expansion over the Eqs. (11), neglecting the elements of higher order in  $S/N$ ,  $1/S$  and  $1/N$ , and substituting the resulting expressions in Eqs. (13) one arrives

to

$$\begin{aligned} \alpha(x) &\approx -\frac{q}{N} \left(1 - \frac{x^2}{2} + \frac{3}{2N}\right), \\ \beta(x) &\approx \frac{-q}{4N^2 x^2} \left(1 - \frac{x^2}{2} + \frac{3}{2N}\right), \\ \gamma(x) &\approx \frac{N}{2} U_S x^2 - qN \left(1 - \frac{x^2}{4} + \frac{1}{2N} + \frac{1}{8N^2 x^2}\right). \end{aligned} \quad (14)$$

We had a general state  $|\phi\rangle = \sum_S c_S |s\rangle$ , whose coefficients have been approximated to a continuous function  $c(x)$  with  $x = S/N$ , as  $S \ll N$ . Performing Taylor expansions and keeping the resulting expressions up to first or second order of the quantities  $1/S$ ,  $S/N$  and  $1/N$ , we have arrived to a continuous expression of the Schrödinger equation and, as a consequence, of the Hamiltonian. It is now convenient to compare these approximated results with the exact ones.

The solution of the exact Schrödinger equation, Eq. (9), has two independent families, even and odd, of solutions as the equation only connects the states in jumps of spin 2. The two solutions, however, are degenerated and have the same shape. For that reason, and taking into account that an even number of particles have been assumed, only the even solution will be considered. The basis  $|S\rangle = |0\rangle, |2\rangle, \dots, |N\rangle$  will be then used, resulting in a  $(N/2 + 1)$ -dimensional space.

Fig. (1) illustrates the comparison between the approximated and the exact Hamiltonian. The approximation for the ground state gives a very good energy although fails to reproduce the shape of the state. The main discrepancy takes place at low values of  $x$ , where the consideration  $1 \ll S \ll N$  is not fulfilled. For the approximated case, the value of  $c(x)$  at the origin always tends to zero due to numerical reasons, while it does not happen the same in the exact solution. This zero value at the origin, modifies the function so the final resulting state has a similar shape, with light discrepancies on the maximum. Nevertheless, as it will be seen later, this does not affect so much the shortcutting procedure.

Further approximations have to be performed for getting an harmonic-like Hamiltonian. This can be done just by neglecting more terms in Eqs. (14). The final expressions are [2]

$$\begin{aligned} \alpha(x) &\approx -\frac{q}{N}, \\ \beta(x) &\approx 0, \\ \gamma(x) &\approx \frac{N}{2} U_S x^2 - qN \left(1 - \frac{x^2}{2}\right). \end{aligned} \quad (15)$$

These approximations may seem too severe, but neither the energy nor the shape are strongly modified. Also, the final result will be highly satisfactory and they are needed for applying the already known shortcut protocols.

The final Schrödinger-like equation is

$$-\frac{q}{N} c''(x) + \frac{N}{4} (q + 2U_S) x^2 c(x) = (E + Nq) c(x). \quad (16)$$

### C. Shortcut protocol to adiabatic evolution

In this section we will derive the approximate method to shortcut the adiabatic evolution for our many-body Hamiltonian (1). The idea is the following, first we consider that the system is initially prepared at time  $t_0 = 0$  in the ground state for a certain initial value of the control parameter, which in our case is  $q(0) = q_i$ . Then, we want that at a given time  $t_f$  the system is exactly in the ground state of the system for a different value of the control parameter,  $q(t_f) = q_f$ . The goal is thus to find a function  $q(t)$  which does the job. If the final time is sufficiently large a linear ramping of the control parameter should work, as the evolution would be essentially adiabatic. In contrast, if the desired final time is made shorter, the linear ramping eventually ceases to work as it produces the excitation of many modes, besides the ground state, at the final time. This problem has been solved exactly for the single-particle harmonic oscillator in Ref. [6]. The protocol obtained there has been adapted to other problems in which a harmonic approximation of the original Hamiltonian is justified [4, 5].

In our case, we have checked that the approximate Schrödinger equation, Eq. (16), reproduces reasonably the full many-body results. Thus, in this section we will first build a harmonic approximation to Eq. (16) which will be valid in a certain range of parameters. Then we will adapt the protocol of Ref. [6] to our problem.

The evolution of the system will be described by the time-dependent Schrödinger equation

$$\hat{H}|\phi\rangle = i\hbar\partial_t|\phi\rangle. \quad (17)$$

The Schrödinger-like equation in Eq. (16) is already very similar to an harmonic oscillator. The QZ energy is our control parameter, so it will change over time,  $q = q(t)$ . It appears three times in the Hamiltonian. However, only one of them is relevant. The term on the right acts only as a shift in the total energy and, although it changes during the evolution, it does not affect to the determination of the equilibrium state. Also, the regime studied is where  $q \ll U_S$ , so  $q$  can be neglected in front of  $U_S$ . Then,  $q + 2U_S \approx 2U_S$ . This may seem a limitation for the Hamiltonian to be  $q$  dominated, but it is not that case. In the exact Hamiltonian,  $U_S$  is divided by  $N$ , so as long as  $q \ll U_S \ll qN$ , the conditions are fulfilled. Even more, when the system is ruled by the quadratic Zeeman energy, it means that most of the particles have the third component of the spin set to zero (see Table 1). Then,  $\langle \hat{N}_0 \rangle \approx N$ , so the conditions become  $q \ll U_S \ll qN^2$ . After all these considerations, the final Schrödinger-like equation is an harmonic oscillator of the form,

$$-\frac{q(t)}{N}c''(x) + \frac{NU_S}{2}x^2c(x) = Ec(x). \quad (18)$$

In Ref. [5], the shortcut protocol has been used for the following Hamiltonian,

$$\hat{\mathcal{H}} = -2J(t)\eta^2\partial_z^2 + \frac{NU}{4}z^2. \quad (19)$$

Hence, applying the following change of variables,

$$q(t) \leftrightarrow 2J(t) \quad (20)$$

$$\frac{1}{N} \leftrightarrow \eta^2 \quad (21)$$

$$U_S \leftrightarrow \frac{U}{2} \quad (22)$$

the control parameter  $J(t)$  can be directly mapped to  $q(t)$ . The shortcut protocol will require some modifications to the Schrödinger-like equation, which finally results in solving the following Ermakov equation,

$$2\frac{(\dot{b})^2}{b} - \ddot{b} + 2NU_Sq(t)b = \frac{k^2}{\eta'^2}b^5, \quad (23)$$

where  $k = NU_S$  and  $\eta' = \sqrt{1/N}$ .  $b(t)$  is an arbitrary function which only has to fulfil the following frictionless conditions,

$$\begin{aligned} b_i \equiv b(t_0) &= \left(\frac{2q(t_0)}{N^2U_S}\right)^{1/4}, \\ b_f \equiv b(t_f) &= \left(\frac{2q(t_f)}{N^2U_S}\right)^{1/4}, \\ \dot{b}(t_0) = \dot{b}(t_f) &= \ddot{b}(t_0) = \ddot{b}(t_f) = 0, \end{aligned} \quad (24)$$

where  $t_0$  will always be zero.

There is an infinite set of functions  $b(t)$  that can be used for this purpose as the boundary conditions leave a lot of freedom. This freedom can be used for controlling other quantities, such as the maximum or minimum value of  $q(t)$  during the evolution or limiting the energy in such a way that the condensate is not heated too much. A polynomial ansatz for  $b(t)$  will be used. Taken from Ref. [4],

$$b(t) = b_i + 10(b_f - b_i)s^3 - 15(b_f - b_i)s^4 + 6(b_f - b_i)s^5, \quad (25)$$

where  $s = t/t_f$ .

## III. RESULTS

The results presented in the previous sections have provided us a recipe to modify our control parameter, ruled by the external magnetic field, for shortcutting the adiabatic evolution. In order to see the improvements of this protocol, it will be constantly compared to a linear variation of the control parameter,  $q$ .

The number of particles used for the simulations has been  $N = 1000$  and the interaction term  $U_S = 10$ . The variation of  $q$  has been from  $q_i \equiv q(0) = 1$ , until values very  $q_f \equiv q(t_f) \simeq 0$ . Then, the initial state will be  $q$ -dominated ( $Nq \gg U_S$ ), which is experimentally easier to prepare. The final state, on the other hand, will have almost no magnetic field applied, so it will be close to the singlet state that we are trying to produce. We will compare the shortcut protocol with the linear variation

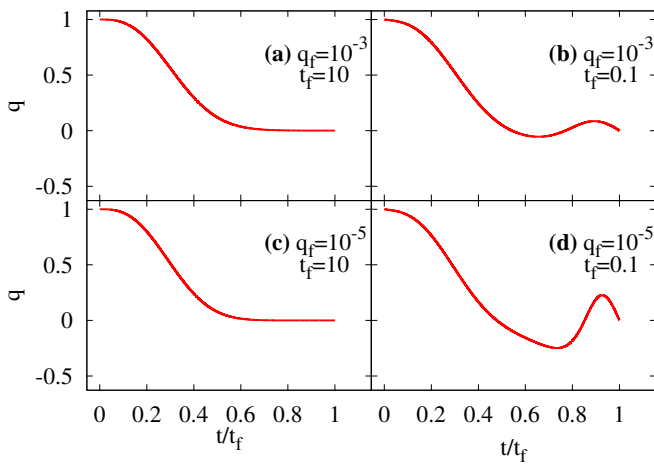


FIG. 2: These plots display the evolution of the QZ energy over time,  $q(t)$ , following the shortcut protocol. Different final times and QZ energy are used: (a)  $q_f = 10^{-3}$  and  $t_f = 10$ ; (b)  $q_f = 10^{-3}$  and  $t_f = 0.1$ ; (c)  $q_f = 10^{-5}$  and  $t_f = 10$ ; (d)  $q_f = 10^{-5}$  and  $t_f = 0.1$ . For all these plots  $N = 1000$ ,  $U_S = 10$  and  $q_i = 1$ .

of the QZ energy from  $q_i$  to  $q_f$ . Depending on the total variation of  $q$ ,  $\Delta q \equiv q_f - q_i$ , and the final time,  $t_f$ , the shortcut protocol can be better or worse than the linear ramping. If the final time is too long or the variation in the QZ energy too little, both methods are almost adiabatic and no difference is observed between them. In the opposite case, for very short time intervals or very large  $\Delta q$ , both methods fail to reproduce the desired final state. Between these two limits, there is a wide region where the shortcut can be a better option than the linear ramping for optimizing the production of the singlet state.

First, it is convenient to study how is the variation of  $q(t)$  imposed by the shortcut protocol, according to Eqs. (23)-(25). The final time and QZ energy are the two variables that will modify the time dependence of  $q$ . In Fig. (2), the shape of  $q(t)$  when the shortcut protocol is applied is shown for different values of  $q_f$  and  $t_f$ . Two different  $q_f$  and  $t_f$  have been used to study the influence of both quantities. In general, if one do not consider very little  $q_f$  or very short times, the variation is smooth, which is suitable for performing experiments. The figure illustrates that for shorter final times, more deviation from the linear ramping is obtained. Equally happens for higher differences between initial and final QZ energies. If  $t_f$  or  $q_f$  are small enough, then  $q$  goes through negative values. However, this situation will not be considered in our calculations.

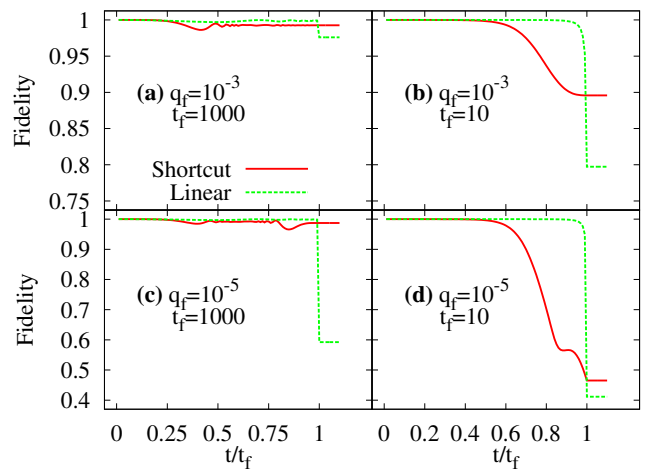


FIG. 3: Here, the overlap between the evolved state and ground state of the Hamiltonian at each time is plotted, also called fidelity. The shortcut protocol and the linear ramping for  $q(t)$  are compared for different  $q_f$  and  $t_f$ : (a)  $q_f = 10^{-3}$  and  $t_f = 1000$ ; (b)  $q_f = 10^{-3}$  and  $t_f = 10$ ; (c)  $q_f = 10^{-5}$  and  $t_f = 1000$ ; (d)  $q_f = 10^{-5}$  and  $t_f = 10$ . For all these plots  $N = 1000$ ,  $U_S = 10$  and  $q_i = 1$ .

#### A. Shortcut protocol applied to the exact Hamiltonian

The shortcut protocol does not have to be, in principle, better than a linear variation for the exact problem, due to all approximations that have been made. By applying the variation of the QZ energy imposed by the previous equations to the exact Hamiltonian we will see whether it is a better option than the linear ramping or not and, therefore, a good method for experimental purposes.

Fig. (3) shows the fidelity during the evolution in four cases, comparing the linear ramping and the shortcut protocol applied to the exact Hamiltonian, as written in Eq. (1). The fidelity here is defined as the overlap between the instantaneous ground state of the Hamiltonian and the actual evolved state,  $\langle \phi_0 | \phi_{\text{evolved}} \rangle$ . This quantity allows us to measure the quality of the final state and the proximity to the adiabatic condition during the evolution of the system.

If the variation of  $q(t)$  is slow enough, the evolution is adiabatic. In this situation, the fidelity is always 1, as the evolved state is at every moment the instantaneous ground state of the system. However, the relevant feature is how close to 1 is the final fidelity, which will mean that the final state is close to the expected one.

Different behaviours are observed for both methods. The shortcut protocol does not follow the adiabaticity as much as the linear ramping during the evolution but reaches a better final state. The fidelity of this final state depends on both  $t_f$  and  $q_f$ . If we stress the conditions by requiring very small values for  $t_f$  and  $q_f$  the performance of both methods worsens. However, in all four cases considered the shortcut protocol gives better results than the

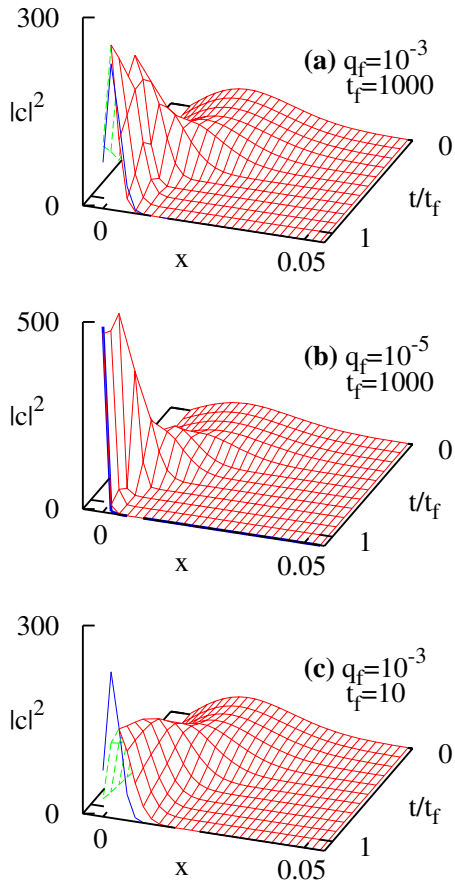


FIG. 4: These plots show the evolution of the state when modifying  $q$  according to the shortcut protocol for different final times and QZ energies: (a)  $q_f = 10^{-3}$  and  $t_f = 1000$ ; (b)  $q_f = 10^{-5}$  and  $t_f = 1000$ ; (c)  $q_f = 10^{-3}$  and  $t_f = 10$ . The final desired state is also plotted. For all these plots  $N = 1000$ ,  $U_S = 10$  and  $q_i = 1$ .

linear ramping.

The shortcut protocol gives better results than the linear ramping when trying to reach states at very small  $q$ . Fidelity one, or close, cannot be achieved for very short time intervals. However, for larger intervals, our protocol achieves very good results while the linear ramping still fails to reproduce the final expected state.

In all cases shown in the figure, the linear ramping is very close to the adiabatic following during the evolution until just the end, where it drops dramatically to a final value. To understand this behaviour, one should notice that the important rate in the Hamiltonian is  $q/U_S$ , so variations in orders of magnitude of  $q$  plays a key role.

The instantaneous ground state of the Hamiltonian varies in a similar amount when  $q$  changes from 1 to 0.1 than when it changes from  $10^{-4}$  to  $10^{-5}$ , as the ratio  $q/U_S$  is modified by the same factor, although the total difference is much lower in the last situation. However, when  $q$  decreases linearly, the variation  $1 \rightarrow 0.1$  lasts

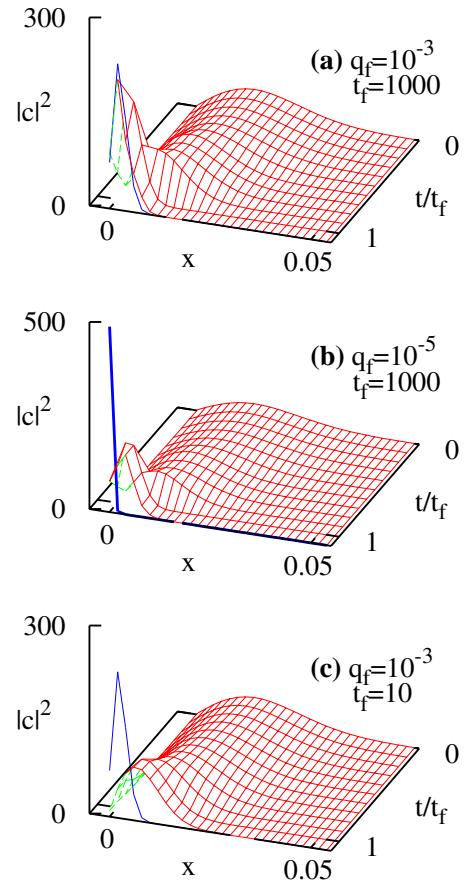


FIG. 5: These plots show the evolution of the state when modifying  $q$  linearly for different final times and QZ energies: (a)  $q_f = 10^{-3}$  and  $t_f = 1000$ ; (b)  $q_f = 10^{-5}$  and  $t_f = 1000$ ; (c)  $q_f = 10^{-3}$  and  $t_f = 10$ . The final desired state is also plotted. For all these plots  $N = 1000$ ,  $U_S = 10$  and  $q_i = 1$ .

$10^4$  times more than the variation  $10^{-4} \rightarrow 10^{-5}$ . Hence, in the last moments of the linear evolution is where the instantaneous ground state changes more. The evolved state, however, does not evolve so rapidly in the end, where the process ceases to be adiabatic. When the QZ energy approaches to zero in the end of the evolution,  $q$  decreases by several orders of magnitude in very short times and the system cannot accommodate so rapidly. As a result, the final state differs substantially from the expected ground state.

When the time interval is small and the variation of the QZ energy is not too large, none of the methods reproduce the final state with fidelity 1, although even here the shortcut model is better. In this situation, although the precision is not as good as for large times, it can be adjusted to have a good enough result (fidelity higher than 0.9 for example).

When  $t_f$  is too short and  $q_f$  is very close to zero, both methods fail to reproduce the final expected state. As can be seen in Fig. (3), the shortcut protocol still pro-

vides better results than the linear ramping, this should not be taken as a general statement. When the interval of time is very short, the shortcut protocol gives  $q(t)$  with very abrupt variations, even passing through negative values, which can lead to a final state worse than the obtained with the linear ramping, although neither of them with good fidelities. There are some cases where the fidelity during the evolution can drop to zero. That usually happens when  $q$  changes sign during the time evolution, which makes the instantaneous ground state to be almost orthogonal to the real evolved state.

Figs. (4) and (5) display the evolution over time of the state when the shortcut protocol and the linear ramping, respectively, have been applied. Three of the cases on Fig. (3) are shown. The final expected state is also plotted. The case where the final fidelity was worse has not been plotted, when  $q_f = 10^{-5}$  and  $t_f = 10$ .

For large evolved times,  $t_f = 1000$ , the shortcut protocol allows the state to achieve a final state very similar to the expected one for both smaller or larger  $\Delta q$ . For the linear case, however, large differences in the QZ energy lead to bad results, as explained above. Actually the linear ramping leads to very similar states when  $q_f = 10^{-3}$  and  $q_f = 10^{-5}$ . As during final times  $q(t)$  decreases several orders of magnitude and the system does not adapt quick enough, for every fixed time the linear variation has a limit state until which it can arrive. Setting lower values of  $q_f$  than the limit value, the system will reach practically the same state. On the other hand, the shortcut protocol contains the information of the expected final state, so the variation of the state is done earlier in time, finishing with a good final fidelity, as can be seen in the figures. If the desired final times are further decreased, the state is not able to evolve fast enough to reach the final state.

In the experimental set-up, one do not want to freeze the dynamics, so it is good to observe what happens right after  $q$  has arrived to its final value. It is preferable that the quantities remain constant after finishing the shortcut protocol (or the linear ramping) because the experiment over the state may not be made instantaneously after the end of the variation, but shortly after.

In Fig. (3) it can be observed that the fidelity remains constant after the QZ energy has arrived to its final value. Nevertheless, not all quantities remain constant after  $t_f$ . The energy is one of them, as the two parts of the Hamiltonian change over time once the protocol has been finished. The value  $\langle S^2 \rangle(t)$ , which is the average value of the total spin operator, is a good quantity to understand this behaviour.

Plotting  $S^2$  over time, see Fig. (6), one observes that, unlike fidelity, it does change after  $q$  has arrived to its final value, for  $t > t_f$ . After  $t_f$ ,  $S^2$  starts to oscillate around a value usually larger than the desired one, as can be seen in Fig. (6b). The amplitude and period of this oscillations depend on  $q$ . Here, the linear ramping leads to oscillations with larger amplitudes than the shortcut protocol. However, in Fig. (6a), the oscillations are not

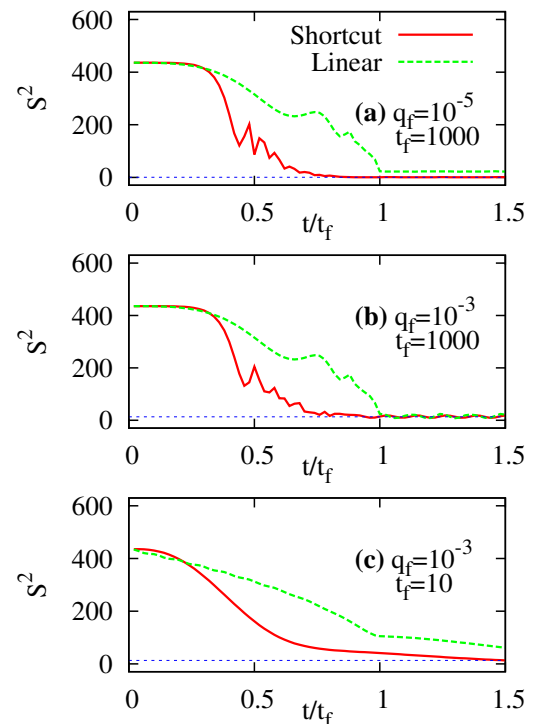


FIG. 6: Here, the average value of the total spin operator,  $\langle S^2 \rangle$  is plotted when  $q$  is varied according to the shortcut protocol and when it is linearly modifying. The comparison is made for different final times and QZ energies: (a)  $q_f = 10^{-5}$  and  $t_f = 1000$ ; (b)  $q_f = 10^{-3}$  and  $t_f = 1000$ ; (c)  $q_f = 10^{-3}$  and  $t_f = 10$ . For all these plots  $N = 1000$ ,  $U_S = 10$  and  $q_i = 1$ .

observed because the amplitude is very little, due to a smaller value of  $q_f$ . Fig. (6c) does not show oscillations as the time is too short to observe them, and only a variation in  $S^2$  for  $t > t_f$  is seen. What is relevant here, is the amplitude and over which value occur the oscillations. In all cases, the shortcut protocol gives a result closer to the expected value and the oscillations right after  $t_f$  are smaller.

The figure of merit,  $|(S^2 - S_{ex}^2)/S_{ex}^2|$ , called relative discrepancy, will be used to see how good the final values of  $S^2$  are by comparing the exact ground state value,  $S_{ex}^2$ , and the actual one at  $t = t_f$ , see Fig. (7). Fig. [7a] shows the discrepancy depending on the final  $q$  for a fixed  $t_f$ . When  $q_f$  is not so close to zero, both methods give good results. As  $q_f$  approaches zero, the performance of the linear ramping deteriorates. In the end, for very small  $q_f$  the relative discrepancy increases also for the shortcut protocol. For that region,  $S^2 \approx 0$ , small values of  $S^2 - S_{ex}^2$  lead to large relative discrepancies.

When the final  $q$  is fixed and the times modified, a similar behaviour is observed. For short enough times, both differ substantially (note the difference in the y-axis between the two plots), although the linear ramping gives better results as the shortcut protocol leads to very



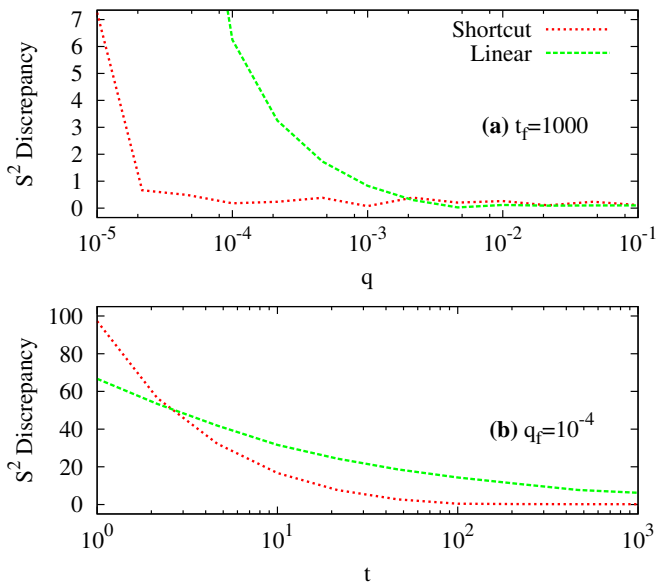


FIG. 7: The plot above, (a), displays the discrepancy in  $S^2$ , which is defined as  $|(S^2 - S_{ex}^2)/S_{ex}^2|$ , for different values of final  $q$ , with  $t_f$  fixed at 1000. In (b), the analogous plot is done but fixing  $q_f$  to  $10^{-4}$  and varying the final time. Note the difference in the y axis. The values  $N = 1000$ ,  $U_S = 10$  and  $q_i = 1$  are used for both plots.

abrupt changes of  $q$ . There is a region where the shortcut is clearly better than the linear ramping. If the time interval is much larger, both methods produce the same good results as the evolution is adiabatic for both. However, with the shortcut method the final times can be reduced by up to three orders of magnitude retaining a good performance.

### B. Realistic values

In this section we will consider experimental values of  $N$ ,  $U_S$ ,  $t_f$  and  $q_f$  taken from Ref.[2]. The experiments have been done between  $10^2 - 10^6$  atoms. Then, the simulations will be made with  $N = 1000$ . The interaction term  $\hbar U_S/k_B$  is around  $5nK$ , which means  $U_S = 104.16s^{-1}$ . The magnetic field and, therefore,  $q$  can be tuned from values much larger than  $U_S$  to zero.

The initial QZ energy has to be lower than  $U_S$  for the approximations made so  $q_i = 0.1U_S$ . Then the initial state has  $Nq = 100U_S$ , so it is very close to the limit case where all bosons are in the  $m = 0$  Zeeman sublevel. The final state, on the other hand, will vary from  $q_f = 10^{-3}U_S$  to  $q_f = 10^{-5}U_S$ . This last value is very close to the singlet state, where  $S = 0$ .

In Fig. (8), the fidelities are displayed in a map for different final times and final QZ energies. The shortcut protocol gives better or equally good results than the linear ramping in all the explored region. Where it gives better results is when  $q_f$  is lower, that means that is

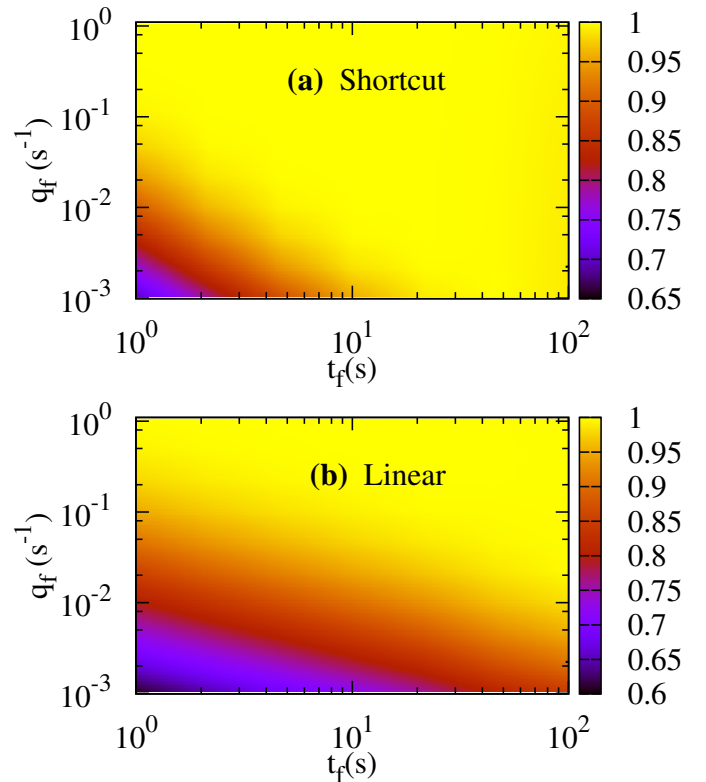


FIG. 8: In this figure the final fidelities of the evolved states are plotted for the case where the shortcut protocol (a) has been followed and when the linear ramping (b) has been used. The fidelities, that is, the overlap between the final evolved state and the desired ground state, are plotted for different final times and QZ energies. The final times and QZ energies are varied along the x and y axis respectively, while the initial  $q$  is set to  $q_i = 0.1U_S = 10.416s^{-1}$ . For both plots  $N = 1000$  and  $U_S = 104.16s^{-1}$ .

better when we are closer to the singlet state. A tendency can be observed and for very small  $q_f$ , the linear ramping needs much higher final times than using the shortcut protocol for obtaining fidelities close to 1. For arriving to the best considered state, which in our case is  $q_f = 10^{-5}$ , following the shortcut protocol it can be done in less than half minute. Using the linear ramping, however, for a good enough state more than 100s should be used. If  $q_f$  is smaller, the difference between two methods increases even more.

For smaller variations of  $q$ , the shortcut protocol still gives better results, although the linear ramping can give good results also. For example, for a difference of only one order of magnitude in  $q$ , that is, from  $0.1U_S$  to  $0.01U_S$ , 1s is more than enough for both methods.

In Fig. (9) we plot the relative discrepancy in the total spin. Comparing the results in Fig. (9) and Fig. (8), we can see that, as expected, fidelities close to 1 correspond to small discrepancies. Let us note that a small decrease in the fidelity, e.g. 0.95, already produce relative discrepancies of the order of 1.

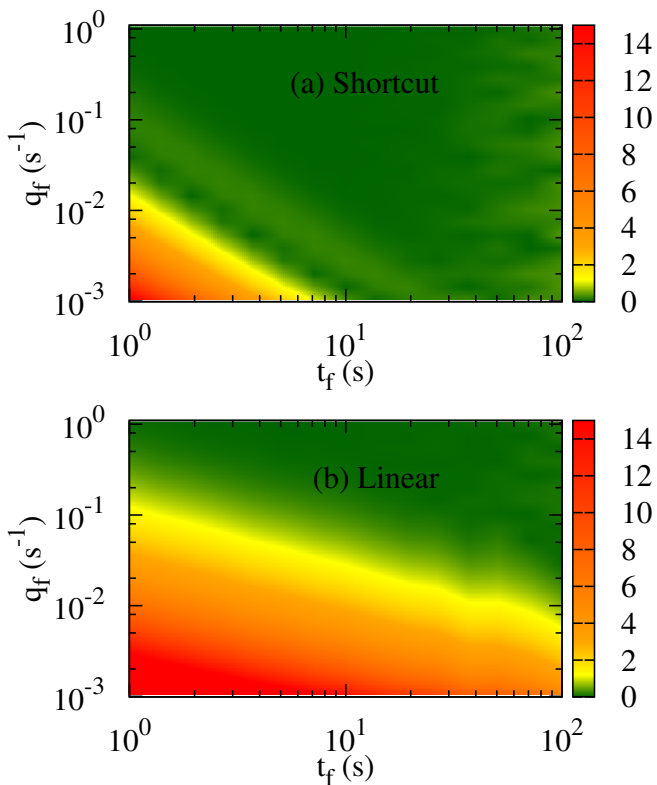


FIG. 9: In this figure the discrepancies between the final and the expected value of  $S^2$  are shown. The figures display the discrepancy in  $S^2$ , which is defined as  $|(S^2 - S_{ex}^2)/S_{ex}^2|$ , of the evolved states, for the case of the shortcut protocol (a) and the linear ramping (b). The final times and QZ energies are varied along the x and y axis respectively, while the initial  $q$  is set to  $q_i = 0.1U_S = 10.416s^{-1}$ . For both plots  $N = 1000$  and  $U_S = 104.16s^{-1}$ .

#### IV. CONCLUSIONS

In this master thesis we have presented a fast protocol for the production of a macroscopic spin singlet state of a spin 1 Bose gas. The initial state of the system is taken to be a BEC where almost all atoms populate the  $m = 0$  Zeeman sublevel. This can be achieved by increasing the quadratic Zeeman shift between the sublevels thus

favoring the condensation on the  $m = 0$  manifold.

We have constructed a basis of states of well defined total spin and obtained the exact discrete Schrödinger equation governing the time evolution of the coefficients of the state in this basis. To produce as final state the spin singlet state we have adapted an exact protocol to shortcut the adiabatic evolution originally developed for a single-particle harmonic oscillator potential. The control parameter used has been the quadratic Zeemann splitting between the levels, which can be tuned externally in current experimental setups. To obtain the protocol, i.e. the variation with time of the control parameter, we have first built a continuum approximation of the exact many-body Schrödinger equation which we have further approximated by a harmonic oscillator potential. Afterwards, we have turned into the original many-body Hamiltonian and have studied the performance of the protocol to produce the macroscopic singlet state comparing it to the result obtained by a linear ramping of the control parameter. This we have done by solving the exact many-body time dependent Schrödinger equation with a time dependent Hamiltonian. The results show that our proposed method provides in almost all situations a better final result than the linear ramping.

The improvement is particularly good when the final desired value of the quadratic Zeemann energy is closer to zero, which is needed to get a many-body state close to the spin singlet. Importantly, the time dependence needed for the control parameter is fairly smooth. This makes it amenable for real experimental setups and allows a fair amount of freedom which could be employed to, e.g. reduce the transient energies or ensure that the control parameter is bound to certain values.

#### V. ACKNOWLEDGEMENTS

I would like to thank Bruno Julià and Artur Polls, who have been of a huge help during the realization of this work, due to the discussions and the orientation provided. I would also like to thank Prof. Fabrice Gerbier, who has provided handwritten notes for the construction of the states and the continuum approximation.

- 
- [1] E. J. Mueller, T. L. Ho, M. Ueda and G. Baym Phys. Rev. A **74**, 033612 (2006).  
 [2] L. De Sarlo, L. Shao, V. Corre, T. Zibold, D. Jacob, J. Dalibard and F. Gerbier New Journal of Physics **15**, 113039 (2013).  
 [3] D. Jacob, L. Shao, V. Corre, T. Zibold, L. De Sarlo, E. Mimoun, J. Dalibard, and F. Gerbier Phys. Rev. A **86**, 061601 (2012).

- [4] B. Julià-Díaz, E. Torrontegui, J. Martorell, J. G. Muga, and A. Polls Physical Review A **86**, 063623 (2012).  
 [5] A. Yuste, B. Julià-Díaz, E. Torrontegui, J. Martorell, J. G. Muga, and A. Polls Physical Review A **88**, 043647 (2013).  
 [6] Xi Chen, A. Ruschhaupt, S. Schmidt, A. del Campo, D. Gury-Odelin, and J. G. Muga Phys. Rev. Lett. **104**, 063002 (2010).